Benjamin–Feir instability of waves in the presence of current

I.V. Shugan, H.H. Hwung, R.Y. Yang
International Wave Dynamics Research Center, National Cheng Kung University,
Tainan, Taiwan,

Abstract

The development of Benjamin–Feir instability of Stokes waves in the presence of variable current is presented. We employ a model of a resonance system having three coexisting nonlinear waves and nonuniform current. ~~The model is free from the narrow-band approximation for surface waves and relatively weak adverse current~~. The model considers essential variations of the wave numbers and frequencies of interacting waves due to significant adverse current rising up to wave blocking value. The modulation instability of Stokes waves in nonuniform moving media has special properties. Interaction with countercurrent accelerates the growth of sideband modes on a short spatial scale. An increase in initial wave steepness intensifies the wave energy exchange accompanied by wave breaking dissipation, results in asymmetry of sideband modes and a frequency downshift with an energy transfer jump to the lower sideband mode, and depresses the higher sideband and carrier wave. Nonlinear waves may even overpass the blocking barrier produced by strong adverse current. The frequency downshift of the energy peak is permanent and the system does not revert to its initial state. We find reasonable correspondence between the results of model simulations and available experimental results for wave interaction with blocking opposing current. Large transient or freak waves with amplitude and steepness several times those of normal waves may form during temporal nonlinear focusing of the resonant waves accompanied by energy income from sufficiently strong opposing current. We employ the resonance model for the estimation of the maximum amplification of wave amplitudes as a function of ~~gradually increasing~~ opposing current value and compare the result obtained with recently published experimental results and modeling results obtained with the nonlinear Schrödinger equation.

KEY WORDS: Frequency downshifting, modulation instability, wave–current interaction, surface waves, rogue waves.

1. Introduction

The problem of the interaction of a nonlinear wave with large-scale current remains an enormous challenge in physical oceanography. In spite of numerous papers devoted to the analysis of the phenomenon, some of the relatively strong effects still await a clear description. The phenomenon can be considered the discrete evolution of the spectrum of the surface wave under the influence of nonuniform adverse current. Experiments conducted by Chavla & Kirby (2002) and Ma et al. (2010) revealed that sufficiently steep surface waves overpass the barrier of strong opposing current on the lower resonant Benjamin–Feir sideband. These reports highlight that the frequency step of a discrete downshift coincides with the frequency step of modulation instability; i.e., after some distance of wave run, the maximum of the wave spectrum shifts in frequency to the lower sideband. The intensive exchange of wave energy produces a peak spectrum transfer jump, which is accompanied by essential wave breaking dissipation. The spectral characteristics of the initially narrow-band nonlinear surface wave packet dramatically change and the spectral width is increased by dispersion induced by the strong nonuniform current.

This paper considers a model of wave resonance in the presence of large-scale variable current with strong emphasis on the development of Benjamin–Feir (BF) instability ~~without restrictions placed on the strength of current and the spectral width of the wave modulation~~.

Modulational instability (BF instability) (Benjamin and Feir, 1967) is a fundamental principle of nonlinear water wave dynamics. This phenomenon is of the utmost importance for the description of dynamics and downshifting of the energy spectrum among sea surface waves, the formation of freak (or giant) waves in oceans and wave breaking. In modern nonlinear physics, BF instability is considered a basic process that classifies the qualitative behavior of modulated waves ("envelope waves") and may initialize the formation of stable entities such as envelope solitons.

The stationary nonlinear Stokes wave is unstable in response to perturbation of two small neighboring sidebands. The initial exponential growth of the two dominant sidebands at the expense of the primary wave gives rise to an intriguing Fermi–Pasta–Ulam recurring phenomenon of the initial state of wave trains. This phenomenon is characterized by a series of modulation–demodulation cycles in which initially uniform wave trains become modulated and then demodulated until they are again uniform (Lake et al., 1978). However, when the initial slope is sufficiently steep, the long-time evolution of the wave train is different. The evolving wave trains experience strong modulations followed by demodulation, but the dominant component is the component at the frequency of the lower sideband of the original carrier. This is the temporary frequency downshift phenomenon. In systematic well-controlled experiments, Tulin and Waseda (1999) analyzed the effect of wave breaking on downshifting, high-frequency discretized energy, and the generation of continuous spectra. Experimental data clearly show that the active breaking process increases the permanent frequency downshift in the latter stages of wave propagation.

The BF instability of Stokes waves and its physical applications have been studied in depth over the last few decades; a long but incomplete list of research is Lo and Mei (1985), Duin (1999), Osborne, Onorato, and Serio (2000), Trulsen et al. (2000), Janssen (2003), Segur et al. (2005), Zakharov et al. (2006), Bridges & Dias (2007), Hwung, Chiang and Hsiao (2007), Chiang and Hwung (2010), Shemer (2010), and Hwung, Chiang, Yang and Shugan (2011). The latter stages of one cycle of the modulation process have been much less investigated, and many physical phenomena that have been observed experimentally still require extended theoretical analysis.

Modulation instability and the nonlinear interactions of waves are strongly affected by variable horizontal currents. Here, we face another fundamental problem of the mechanics of water waves—interactions with long-scale current. The effect of opposing current on waves is a problem of practical importance at tidal inlets and river mouths.

Even linear refraction of waves on currents can affect the wave field structure in terms of the direction and magnitude of waves. Waves propagating against an opposing current may have reduced wavelength and increased wave height and steepness.

If the opposing current is sufficiently strong, then the absolute group wave velocity in the stationary frame will become zero, resulting in the waves being blocked. This is the most intriguing phenomenon in the problem of wave–current interaction (Phillips, 1977). The kinematics condition for wave blocking can be written as

$$C_g + U(X) \to 0,$$

where C_g is the intrinsic group velocity of waves in a moving frame and $U(X)$ is slowly varying horizontal current, with X being the horizontal coordinate in the direction of wave propagation. Waves propagating against opposing current are stopped if the magnitude of the current, in the direction of wave propagation, exceeds the group velocity of the oncoming waves. This characteristic feature of wave blocking has drawn the interest of oceanographers and coastal engineers alike for its ability to be used as signature patterns of underlying large-scale motion (e.g., fresh water plumes and internal waves) and for the navigational hazard it poses. Smith (1975), Peregrine (1976), and Lavrenov (1998) analyzed refraction/reflection around a blocking region and obtained a uniformly valid linearized solution, including a short reflecting wave.

The linear modulation model has a few serious limitations. The most important is that the model predicts the blocking point according to the linear dispersion relation and cannot account for nonlinear dispersive effects. Amplitude dispersion effects can considerably alter the location of wave blocking predicted by linear theory, and nonlinear processes can adversely affect the dynamics of the wave field beyond the blocking point.

Donato, Peregrine & Stocker (1999), Stocker & Peregrine (1999), and Moreira & Peregrine (2012) conducted fully nonlinear computations to analyze the behavior of a train of water waves in deep water when meeting nonuniform currents, especially in the region where linear solutions become singular. The authors employed spatially periodic domains in numerical study and showed that adverse currents induce wave steepening and breaking. A strong increase in wave steepness is observed within the blocking region, leading to wave breaking, while wave amplitudes decrease beyond this region. The nonlinear wave properties reveal that at least some of the wave energy that builds up within the blocking region can be released in the form of partial reflection (which applies to very gentle waves) and wave breaking (even for small-amplitude waves).

The enhanced nonlinear nature of sideband instabilities in the presence of strong opposing current has also been confirmed by experimental observations. Chavla & Kirbi (2002) experimentally showed that the blockage phenomenon strongly depends on the initial wave steepness; i.e., waves are blocked when the initial slope is gradual ($ak < 0.16$, where a and k are the wave amplitude and wave number, respectively). When the slope is sufficiently steep ($ak > 0.22$), the behavior of waves is principally different; i.e., waves are blocked only partly and frequency-downshifted waves overpass the blocking barrier. The lower sideband mode may dramatically increase; i.e., the amplitude may increase several times within a distance of a few wavelengths.

Wave propagation against nonuniform opposing currents was recently investigated in experiments conducted by Ma et al. (2010). Results confirm that opposing current not only increases the wave steepness but also shortens the wave energy transfer time and accelerates the development of sideband instability. A frequency downshift, even for very gradual initial steepness, was identified. Because of the frequency downshift, waves are more stable and have the potential to grow higher and propagate more quickly. The ultimate frequency downshift increases with an increase in initial steepness.

The wave modulation instability with coexisting variable current is commonly described theoretically by employing different forms of the modified nonlinear Schrödinger (NLS) equation. Gerber (1987) used the variational principle to derive a cubic Schrödinger equation for a nonuniform medium, limiting to potential theory in one horizontal dimension. Stocker & Peregrine (1999) extended the modified nonlinear NLS equation of Dysthe (1979) to include a prescribed potential current. Hjelmervik and Trulsen (2009) derived an NLS equation that includes waves and currents in two horizontal dimensions allowing weak horizontal shear. The horizontal current velocities are assumed just small enough to avoid collinear blocking and reflection of the waves.

Even though the frequency downshift and other nonlinear phenomena were observed in previous experimental studies on wave–current interactions, the theoretical description of the modulation instability of waves on opposing currents is not yet complete. An interaction of an initially relatively steep wave train with strong current nevertheless may abruptly transfer energy between the resonantly interacting harmonics. Such wave phenomena are beyond the applicability of NLS-type models and await a theoretical description.

Another topic of practical interest in wave–current interaction problems is the appearance of large transient or freak waves with great amplitude and steepness owing to the focusing mechanism (e.g., Peregrine (1976); Lavrenov (1998), White & Fornberg (1998), Kharif and Pelinovsky (2006); Janssen and Herbers (2009), Ruban (2012)). Both nonlinear instability and refractive focusing have been identified as mechanisms for extreme-wave generation and these processes are generally concomitant in oceans and potentially act together to create giant waves.

Toffoli et al. (2013) showed experimentally that an initially stable surface wave can become modulationally unstable and even produce freak or giant waves when meeting negative horizontal current. Onorato *et al.* (2011) suggested an equation for predicting the maximum amplitude $A_{\max}$ during the wave evolution of currents in deep water. Their numerical results revealed that the maximum amplitude of the freak wave depends on U/c_g, where U is the velocity of the current and c_g is the group velocity of the wave packet.

Recently, Ma et al. (2013) experimentally investigated the maximum amplification of the amplitude of a wave on opposing current having variable strength at an intermediate water depth. They mentioned that theoretical values of amplification (Onorato *et al.* (2011), Toffoli et al. (2013)) are essentially overestimated, probably owing to the effects of finite depth and wave breaking.

To address the abovementioned problems, we present a third-order resonance model of BF instability in the presence of horizontal long-scale current of variable strength. We analyze the interactions of a nonlinear surface wave with sufficiently strong opposing blocking current and the frequency downshifting phenomenon. The maximum amplification of the amplitude of surface waves is estimated ~~for gradually increasing~~ in dependence from relative strength of opposing current. We take into account the dissipation effects due to wave breaking and explore the threshold modification of the Tulin wave breaking model (Tulin (1996); Huang et al. (2011)). The results of model simulations are compared with available experimental results and theoretical estimations.

We employ simplified 3-wave quasi-resonance model in the presence of significant opposite current. In the meanwhile, the evolution of the wave spectrum in the absence of breaking includes energy exchange between the carrier wave and two main resonant side-bands and spreading of the energy to higher frequencies. Inclusion of higher frequency free waves in the Zakharov, modified Schrodinger or Dysthe equations is crucial, since the asymmetry of the lower and the upper side-band amplitudes at peak modulation in non-breaking case results from that. The temporal spectral downshift has been predicted by computations made by the Dysthe equations (Lo and Mei, 1985; Trulsen and Dysthe, 1990; Hara and Mei, 1991) for a much more number of excited waves, the same prediction was also made by simulations of fully nonlinear equations (Tanaka,1990; Slunyaev and Shrira, 2013). Such a conclusion can be made regarding to developing of modulation instability in a calm water.

The developing of modulation instability in the presence of significant adverse current is different. Experimental results of Chavla and Kirby (2002) and Ma et al. (2010) clearly show that energy spectrum is mostly concentrated in the main triad of waves and high frequency discretized energy spreading is depressed due to the short wave blocking by the strong enough adverse current.

The relatively high initial wave steepness leads to wave breaking dissipation with discriminatory energy loss from the carrier and higher side-band modes (Tulin and Waseda, 1999). Even those waves which do not blocked lose a considerable amount of energy due to wave breaking on the strong opposite current. The permanent frequency downshift with final dominating of the lower subharmonic takes a place and wave system does not revert to its initial state. 3-wave dynamical model analysis in the presence of significant opposite current therefore can be relevant at the initial stages and also at the further stages of wave evolution.

The paper consists of five sections. General modulation equations that describe the one-dimensional interaction of a triad of resonant surface waves and nonuniform current are derived in section 2. Section 3 analyzes stationary nondissipative solutions for adverse and following nonuniform currents and various initial steepness of the surface wave train. We calculate the maximum amplitude amplification ~~along gradually increasing~~ in dependence from relative strength of opposing current and compared it with available experimental and theoretical results (Toffoli et al., 2013; Ma et al., 2013). The interaction of steep surface waves with strong adverse current under wave-blocking conditions including wave breaking effects is presented in section 4. Modeling results are compared with the results of a series of experiments conducted by Chavla and Kirby (2002) and Ma et al. (2010). Section 5 summarizes our final conclusions and discussion.

2. Modulation equations for one-dimensional interaction

The first set of complete equations that describe short waves propagating over nonuniform currents of much larger scale were given by Longuet-Higgins and Stewart (1964). Wave energy is not conserved, and the concept of "radiation stress" was introduced to describe the average momentum flux in terms that govern the interchange of momentum with the current. In this model, it is also justifiable to neglect the effect of momentum transfer on the form of the surface current because it is an effect of the highest order (Stocker and Peregrine, 1999).

We construct a model of the current effect on the modulation instability of a nonlinear Stokes wave by making the following assumptions.

i). Surface waves and current propagate along a common *x*-direction.

ii). By a_c, k_c and ω_c we denote the characteristic amplitude, wave number and angular frequency of the surface waves. We use a small conventional average wave steepness parameter; $\varepsilon = a_c k_c << 1$.

iii) The characteristic spatial scale used in developing the BF instability of the Stokes wave is l_c / ε^2, where $l_c = 2\pi / k_c$ is the typical wavelength of surface waves (Benjamin and Feir, 1967). We consider long-scale slowly varying current $U(x)$ with horizontal length scale L of the same order: $L = O(l_c / \varepsilon^2)$.

iv) It is assumed that the $U(x)$ dependence is due to the inhomogeneity of the bottom profile $h(x)$, which is sufficiently deep so that the deep-water regime for surface waves is ensured; i.e., $exp(-2k_c h) \ll 1$. The characteristic current length L at which the function $U(x)$ varies noticeably is assumed to be much larger than the depth of the fluid, $h(x) \ll L$. Under these conditions, shallow water model for the current description may be adopted: $U(x)h(x)$ assumed to be approximately constant, and the vertical component of the steady velocity field on the surface $z = \eta(x)$ can be neglected. Correspondingly, it follows from the Bernoulli time-independent equation that the surface displacement induced by the current is small (Ruban, 2012). Such a situation can occur, for example, near river mouths or in tidal/ebb currents.

In all following equations, variables and sizes are scaled according to the above assumptions, and made dimensionless using the characteristic length and time scales of the wave field.

The zero-dimensional set of equations for potential motion of an ideal incompressible deep-depth fluid with a free surface in the presence of current $U(x)$ is given by the Laplace equation:

$$\phi_{xx} + \phi_{zz} = 0, \ -h(x) < z < \varepsilon\eta(x,t). \qquad (1)$$

The boundary conditions at the free surface are

$$-\eta = \phi_t + U\phi_x + \varepsilon \frac{1}{2}(\phi_x^2 + \phi_z^2), z = \varepsilon\eta(x,t), \tag{2}$$

$$\eta_t + U\eta_x + \varepsilon\phi_x\eta_x = \phi_z, z = \varepsilon\eta(x,t), \tag{3}$$

and those at the bottom are

$$\phi \to 0, z = -h(x). \tag{4}$$

Here, $\phi(x,z,t)$ is the velocity potential, $\eta(x,t)$ is the free-surface displacement, z is the vertical coordinate directed upward and t is time.

The variables are normalized as

$$\begin{aligned} &\phi = a_c\sqrt{\frac{g}{k_c}}\phi' = \varepsilon\sqrt{\frac{g}{k_c^3}}\phi', \eta = a_c\eta' = \frac{\varepsilon}{k_c}\eta', \\ &t = \frac{1}{\sqrt{gk_c}}t', z = \frac{z'}{k_c}, x = \frac{x'}{k_c}, \\ &U(Kx) = U'(K/k_c\ x')c_p = U'(\varepsilon^2 x')c_p, \end{aligned} \tag{5}$$

where g is acceleration due to gravity, $K = 2\pi/L$, and c_p is the phase speed of the carrier wave, but the primes are omitted in equations (1)–(4). Note that normalization (5) explicitly specifies the principal scales of sought functions ϕ and η.

The weakly nonlinear surface wave train is described by a solution to equations (1)–(4), expanded into a Stokes series in terms of ε.

We will analyze the surface wave train as the almost-resonance wave triad of a particular form, which describes the development of modulation instability in the presence of current.

For calm water, the initially constant nonlinear Stokes wave with amplitude, wave number and frequency (a_1, k_1, σ_1) is unstable in response to a perturbation in the form of a pair small waves with similar frequencies and wavenumbers: a superharmonic wave ($a_2, k_2 = k_1 + \Delta k, \sigma_2 = \sigma_1 + \Delta\sigma$) and subharmonic wave ($a_0, k_0 = k_1 - \Delta k, \sigma_0 = \sigma_1 - \Delta\sigma$). For most unstable modes, $\Delta\sigma/\sigma_1 = \varepsilon$ and $\Delta k/k_1 = 2\varepsilon$, where $\varepsilon = a_1 k_1$ is the initial steepness of the Stokes wave (Benjamin and Feir, 1967). This is the BF or modulation instability of the Stokes wave.

Kinematics resonance conditions for waves in the presence of slowly variable current are the same with one important particularity that intrinsic wave numbers and frequencies of resonance waves in the moving frame are variable and modulated by the current.

We analyze the problem assuming the wave motion phase $\theta_i = \theta_i(x,t)$ exists for each resonance wave in the presence of a slowly varying current $U(x)$, and we define the local wave number k_i and absolute observed frequency ω_i as

$$k_i = (\theta_i)_x, \omega_i = \sigma_i + k_i U = -(\theta_i)_t, \\ i = 0,1,2. \tag{6}$$

For stationary modulation, the intrinsic frequency σ_i and wave number k_i for each wave slowly change in the presence of variable current, but the resonance condition

$$2\omega_1 \approx \omega_0 + \omega_2 \tag{7}$$

remains valid throughout the region of wave propagation owing to the stationary value of the absolute frequency for each of the harmonics.

The main kinematics wave parameters (σ_i, k_i) together with the first-order velocity potential amplitudes, ϕ_i, are considered further as slowly varying functions with typical scale, $O(\varepsilon^{-1})$, longer than the primary wavelength and period (Whitham, 1974):

$$\phi_i = \phi_i(\varepsilon x, \varepsilon t), k_i = k_i(\varepsilon x, \varepsilon t), \sigma_i = \sigma_i(\varepsilon x, \varepsilon t). \tag{8}$$

On this basis, we attempt to recover the effects of long-scale current and nonlinear wave dispersion (having the same order) additional to the Stokes term with the order of wave steepness squared.

The solution to the problem, uniformly valid for $O(\varepsilon^3)$, is found by a two-scale expansion with the differentiation:

$$\frac{\partial}{\partial t} = -\sum (\sigma_i + k_i U)\frac{\partial}{\partial \theta_i} + \varepsilon \frac{\partial}{\partial T}, \\ \frac{\partial}{\partial x} = \sum k_i \frac{\partial}{\partial \theta_i} + \varepsilon \frac{\partial}{\partial X}, T = \varepsilon t, X = \varepsilon x. \tag{9}$$

Substitution of the wave velocity potential in its linear form,

$$\phi = \sum_{i=0}^{i=2} \phi_i e^{k_i z} \sin\theta_i , \tag{10}$$

satisfies the Laplace equation (1) to the first order of ε owing to (8) and gives the additional terms of the second order $O(\varepsilon^2)$:

$$\varepsilon(2k_i\phi_{iX} + k_{iX}\phi_i + 2k_i k_{iX}\phi_i z)e^{k_i z}\cos\theta_i + \ldots = 0 \quad .$$

To satisfy the Laplace equation to second order, Yuen and Lake (1982), Shugan and Voliak (1998), and Hwung, Yang and Shugan (2009) suggested an additional phase-shifted term with a linear and quadratic *z* correction in the representation of the potential function ϕ:

$$\phi = \sum_{i=0}^{i=2}\left(\phi_i e^{k_i z}\sin\theta_i - \varepsilon\left(\phi_{iX} z + \frac{k_{iX}\phi_i}{2}z^2\right)e^{k_i z}\cos\theta_i\right) + \ldots . \tag{11}$$

Exponential decaying of the wave's amplitude with increasing –*z* is accompanied by a second-order subsurface jet owing to slow horizontal variations in the wave number and amplitude of the wave packet.

The free-surface displacement $\eta = \eta(x,t)$ is also sought as an asymptotic series:

$$\eta = \eta_0 + \varepsilon\eta_1 + \varepsilon^2\eta_2 + \ldots, \tag{12}$$

where η_0, η_1, and η_2 are $O(1)$ functions to be determined. Using expressions (10) and (11) subject to the dynamic boundary condition (2), we find the components of the free-surface displacement:

$$\eta_0 = \sum_{i=0}^{i=2}\sigma_i\phi_i\cos\theta_i, \tag{13}$$

$$\begin{aligned}\eta_1 = &-\sum_{i=0}^{i=2}(\phi_{iT}\sin\theta_i + U\phi_{iX}\sin\theta_i) + \sum_{i=0}^{i=2}\phi_i^2 k_i^2\cos[2\theta_i]/2 + \\ &\sum_{i=0}^{i=2}\sum_{j\neq i}^{j=2}(\sigma_i - \sigma_j)^2\sigma_i\sigma_j\ \phi_i\phi_j\cos[\theta_i - \theta_j]/2 + \sum_{i=0}^{i=2}\sum_{j\neq i}^{j=2}(\sigma_i + \sigma_j)^2\sigma_i\sigma_j\ \phi_i\phi_j\cos[\theta_i + \theta_j]/2\end{aligned}, \tag{14}$$

$$-8\eta_2 = \begin{pmatrix} \phi_0\sigma_0^2(3\phi_0^2\sigma_0^5 + 2\phi_1^2\sigma_1^2(2\sigma_1^2 + \sigma_0^2)(2\sigma_1 - \sigma_0) + 2\phi_2^2\sigma_2^2(2\sigma_2^2 + \sigma_0^2)(2\sigma_2 - \sigma_0))\cos[\theta_0] + \\ \phi_1\sigma_1^2(3\phi_1^2\sigma_1^5 + 2\phi_0^2\sigma_0^2(2\sigma_0^2 + \sigma_1^2)(2\sigma_0 - \sigma_1) + 2\phi_2^2\sigma_2^2(2\sigma_2^2 + \sigma_1^2)(2\sigma_2 - \sigma_1))\cos[\theta_1] + \\ \phi_2\sigma_2^2(3\phi_2^2\sigma_2^5 + 2\phi_1^2\sigma_1^2(2\sigma_1^2 + \sigma_2^2)(2\sigma_1 - \sigma_2) + 2\phi_0^2\sigma_0^2(2\sigma_0^2 + \sigma_2^2)(2\sigma_0 - \sigma_2))\cos[\theta_2] - \\ \phi_0\phi_1^2\sigma_0\sigma_1^2(\sigma_0^2 + 2\sigma_1^2)(\sigma_0^2 - 4\sigma_0\sigma_1 + 2\sigma_1^2)\cos[\theta_2 + \varphi] - \phi_1^2\phi_2\sigma_1^2\sigma_2(\sigma_2^2 + 2\sigma_1^2)(\sigma_2^2 - 4\sigma_2\sigma_1 + 2\sigma_1^2)\cos[\theta_0 + \varphi] \\ -2\phi_0\phi_1\phi_2\sigma_0\sigma_1\sigma_2(\sigma_0^2 + \sigma_1^2 + \sigma_2^2)(\sigma_0^2 - 2\sigma_0\sigma_1 + \sigma_1^2 - 2\sigma_1\sigma_2 + \sigma_2^2)\cos[\theta_1 - \varphi] \end{pmatrix}, \tag{15}$$

where φ is a slowly varying phase-shift difference: $\varphi = 2\theta_1 - \theta_0 - \theta_2$.

Only the resonance terms for all three wave modes are included in the third-order displacement (15).

Substitution of the velocity potential (11) and displacement (13)–(15) into the kinematics boundary condition (3) gives, after much routine algebra, relationships between the modulation characteristics of the resonant wave:

$$\begin{cases} \sigma_0^2 = k_0 + \varepsilon^2 \sigma_0^3 (\phi_0^2 \sigma_0^5 + \phi_1^2 \sigma_1^3 (2\sigma_1^2 - \sigma_0\sigma_1 + \sigma_0^2) + \phi_2^2 \sigma_2^3 (2\sigma_2^2 - \sigma_0\sigma_2 + \sigma_0^2)) + \\ \dfrac{\varepsilon^2 \phi_1^2 \phi_2 \sigma_1^3 \sigma_2^2}{\phi_0} (2\sigma_1^3 - 2\sigma_1^2\sigma_2 + 2\sigma_1\sigma_2^2 - \sigma_2^3) \cos[\varphi]; \\ \sigma_2^2 = k_2 + \varepsilon^2 \sigma_2^3 (\phi_2^2 \sigma_2^5 + \phi_0^2 \sigma_0^3 (2\sigma_0^2 - \sigma_0\sigma_2 + \sigma_2^2) + \phi_1^2 \sigma_1^3 (2\sigma_1^2 - \sigma_1\sigma_2 + \sigma_2^2)) + \\ \dfrac{\varepsilon^2 \phi_1^2 \phi_0 \sigma_1^3 \sigma_0^2}{\phi_2} (2\sigma_1^3 - 2\sigma_0\sigma_1^2 + 2\sigma_0^2\sigma_1 - \sigma_0^3) \cos[\varphi]; \\ \sigma_1^2 = k_1 + \varepsilon^2 \sigma_1^3 (\phi_1^2 \sigma_1^5 + \phi_0^2 \sigma_0^3 (2\sigma_0^2 - \sigma_0\sigma_1 + \sigma_1^2) + \phi_2^2 \sigma_2^3 (\sigma_1^2 - \sigma_1\sigma_2 + 2\sigma_2^2)) + \\ \varepsilon^2 \phi_0 \phi_2 \sigma_0 \sigma_1^2 \sigma_2 (\sigma_0^4 - \sigma_0^3\sigma_1 - \sigma_0\sigma_1(\sigma_1 - \sigma_2)^2 + \\ \sigma_0^2(\sigma_1^2 - \sigma_1\sigma_2 + 2\sigma_2^2) + \sigma_2(-\sigma_1^3 + \sigma_1^2\sigma_2 - \sigma_1\sigma_2^2 + \sigma_2^3)) \cos[\varphi]; \end{cases} \tag{16}$$

$$\begin{cases} [\phi_0^2\sigma_0^2]_T + [(U(X) + \dfrac{1}{2\sigma_0})\phi_0^2\sigma_0^2]_X = \varepsilon\phi_1^2\phi_2\phi_0\sigma_1^3\sigma_2^2(2\sigma_1^3 - 2\sigma_1^2\sigma_2 + 2\sigma_1\sigma_2^2 - \sigma_2^3)\,\mathrm{Sin}[\varphi] - \phi_0^2\sigma_0 U'(X)/2; \\ [\phi_2^2\sigma_2^2]_T + [(U(X) + \dfrac{1}{2\sigma_2})\phi_2^2\sigma_2^2]_X = \varepsilon\phi_1^2\phi_2\phi_0\sigma_0^2\sigma_1^3(2\sigma_1^3 - 2\sigma_0\sigma_1^2 + 2\sigma_0^2\sigma_1 - \sigma_0^3)\,\mathrm{Sin}[\varphi] - \phi_2^2\sigma_2 U'(X)/2; \\ [\phi_1^2\sigma_1^2]_T + [(U(X) + \dfrac{1}{2\sigma_1})\phi_1^2\sigma_1^2]_X = -\varepsilon\phi_1^2\phi_2\phi_0\sigma_0\sigma_1^2\sigma_2(\sigma_0^4 - \sigma_0^3\sigma_1 - \sigma_0\sigma_1(\sigma_1 - \sigma_2)^2 + \\ +\sigma_0^2(\sigma_1^2 - \sigma_1\sigma_2 + 2\sigma_2^2) - \sigma_2(\sigma_1^3 - \sigma_1^2\sigma_2 + \sigma_1\sigma_2^2 - \sigma_2^3))\,\mathrm{Sin}[\varphi] - \phi_1^2\sigma_1 U'(X)/2. \end{cases} \quad \cancel{(17)}$$

$$\begin{cases} [\phi_0^2\sigma_0]_T + [(U(X) + \dfrac{1}{2\sigma_0})\phi_0^2\sigma_0]_X = \varepsilon\phi_1^2\phi_2\phi_0\sigma_1^3\sigma_2^2(2\sigma_1^3 - 2\sigma_1^2\sigma_2 + 2\sigma_1\sigma_2^2 - \sigma_2^3)\,\mathrm{Sin}[\varphi]; \\ [\phi_2^2\sigma_2]_T + [(U(X) + \dfrac{1}{2\sigma_2})\phi_2^2\sigma_2]_X = \varepsilon\phi_1^2\phi_2\phi_0\sigma_0^2\sigma_1^3(2\sigma_1^3 - 2\sigma_0\sigma_1^2 + 2\sigma_0^2\sigma_1 - \sigma_0^3)\,\mathrm{Sin}[\varphi]; \\ [\phi_1^2\sigma_1]_T + [(U(X) + \dfrac{1}{2\sigma_1})\phi_1^2\sigma_1]_X = -\varepsilon\phi_1^2\phi_2\phi_0\sigma_0\sigma_1^2\sigma_2(\sigma_0^4 - \sigma_0^3\sigma_1 - \sigma_0\sigma_1(\sigma_1 - \sigma_2)^2 + \\ +\sigma_0^2(\sigma_1^2 - \sigma_1\sigma_2 + 2\sigma_2^2) - \sigma_2(\sigma_1^3 - \sigma_1^2\sigma_2 + \sigma_1\sigma_2^2 - \sigma_2^3))\,\mathrm{Sin}[\varphi]; \end{cases} \tag{17}$$

The formulas (16) represent the "intrinsic" dispersion relations of the nonlinear wave for each of the resonant harmonics in the presence of current, *U(X)*. Equation (17) yields the known wave ~~energy~~

action law with the energy exchange terms~~ and sink/source term of the wave obtained from the current variability~~ on the right side of the equations.

The obtained system of equations (16), (17) in the absence of current is similar to classical Zakharov equations for discrete wave interactions (Mei et al., 2009); it has a strong symmetry with respect to indexes 0 and 2. The main property of the derived modulation equations is the variability of interaction coefficients in the presence of variable current.

Modulation equations (16) and (17) are closed by the equations of wave phase conservation that follow from (6) as the compatibility condition (Phillips, 1977):

$$\begin{aligned} &k_{iT} + (\sigma_i + k_i U)_X = 0, \\ &i = 0,1,2. \end{aligned} \tag{18}$$

The derived set of nine modulation equations (16)–(18) form the complete system for nine unknown functions ($k_i, \sigma_i, \phi_i, i = 0,1,2$).

3. Nondissipative stationary-wave modulations

Let us analyze the stationary-wave solutions of the problem (16)–(18) supposing that all unknown functions depend on the single coordinate *X*. Then, after integrating (18), we have the conservation law for the absolute frequency of each wave:

$$\begin{aligned} &\sigma_i + k_i U = \omega_i = const, \\ &i = 0,1,2. \end{aligned} \tag{19}$$

The wave ~~energy~~ action laws for resonant components take the form

$$\begin{cases} [(U + \dfrac{1}{2\sigma_0})\phi_0^2\sigma_0^2]_X = \varepsilon\phi_1^2\phi_2\phi_0\sigma_1{}^3\sigma_2{}^2(2\sigma_1{}^3\text{-}2\sigma_1{}^2\sigma_2\text{+}2\,\sigma_1\sigma_2{}^2\text{-}\sigma_2{}^3)\,\sin[\varphi]\text{-}\phi_0^2\sigma_0 U'(X)/2 \\ [(U + \dfrac{1}{2\sigma_2})\phi_2^2\sigma_2^2]_X = \varepsilon\phi_1^2\phi_2\phi_0\sigma_1{}^3\sigma_0{}^2(2\sigma_1{}^3\text{-}2\sigma_0\sigma_1{}^2\text{+}2\sigma_0{}^2\sigma_1\text{-}\sigma_0{}^3)\,\sin[\varphi]\text{-}\phi_2^2\sigma_2 U'(X)/2 \\ [(U + \dfrac{1}{2\sigma_1})\phi_1^2\sigma_1^2]_X = -\varepsilon\phi_1^2\phi_2\phi_0\sigma_0\sigma_1{}^2\sigma_2(\sigma_0{}^4 - \sigma_0{}^3\sigma_1 - \sigma_0\sigma_1(\sigma_1\text{-}\sigma_2)^2 + \\ \sigma_0{}^2(\sigma_1{}^2\text{-}\sigma_1\sigma_2\text{+}2\sigma_2{}^2)\text{-}\sigma_2(\sigma_1{}^3\text{-}\sigma_1{}^2\sigma_2\text{+}\sigma_1\sigma_2{}^2\text{-}\sigma_2{}^3))\sin[\varphi]\text{-}\phi_1^2\sigma_1 U'(X)/2 \end{cases} \qquad \cancel{(20)}$$

$$\begin{cases} [(U+\dfrac{1}{2\sigma_0})\phi_0^2\sigma_0]_X = \varepsilon\phi_1^2\phi_2\phi_0\sigma_1{}^3\sigma_2{}^2(2\sigma_1{}^3\text{-}2\sigma_1{}^2\sigma_2+2\ \sigma_1\sigma_2{}^2\text{-}\sigma_2{}^3)\ \mathrm{Sin}[\varphi] \\ [(U+\dfrac{1}{2\sigma_2})\phi_2^2\sigma_2]_X = \varepsilon\phi_1^2\phi_2\phi_0\sigma_1{}^3\sigma_0{}^2(2\sigma_1{}^3\text{-}2\sigma_0\sigma_1{}^2+2\sigma_0{}^2\sigma_1\text{-}\sigma_0{}^3)\ \mathrm{Sin}[\varphi] \\ [(U+\dfrac{1}{2\sigma_1})\phi_1^2\sigma_1]_X = -\varepsilon\phi_1^2\phi_2\phi_0\sigma_0\sigma_1{}^2\sigma_2(\sigma_0{}^4-\sigma_0{}^3\sigma_1-\sigma_0\sigma_1(\sigma_1\text{-}\sigma_2)^2+ \\ \sigma_0{}^2(\sigma_1{}^2\text{-}\sigma_1\sigma_2+2\sigma_2{}^2)\text{-}\sigma_2(\sigma_1{}^3\text{-}\sigma_1{}^2\sigma_2+\sigma_1\sigma_2{}^2\text{-}\sigma_2{}^3))\mathrm{Sin}[\varphi] \end{cases} \tag{20}$$

To perform the qualitative analysis of the stationary problem, we suggest the law of wave action conservation flux in a slowly moving media as analogue of the three Manley-Rowe dependent integrals:

$$\begin{cases} \left(U+\dfrac{1}{2\sigma_2}\right)\phi_2^2\sigma_2+\left(U+\dfrac{1}{2\sigma_0}\right)\phi_0^2\sigma_0+\left(U+\dfrac{1}{2\sigma_1}\right)\phi_1^2\sigma_1 = const; \\ \dfrac{1}{2}\left(U+\dfrac{1}{2\sigma_1}\right)\phi_1^2\sigma_1+\left(U+\dfrac{1}{2\sigma_0}\right)\phi_0^2\sigma_0 = const; \\ \dfrac{1}{2}\left(U+\dfrac{1}{2\sigma_1}\right)\phi_1^2\sigma_1+\left(U+\dfrac{1}{2\sigma_2}\right)\phi_2^2\sigma_2 = const; \\ \left(U+\dfrac{1}{2\sigma_0}\right)\phi_0^2\sigma_0-\left(U+\dfrac{1}{2\sigma_2}\right)\phi_2^2\sigma_2 = const. \end{cases}$$

These integrals follow from the system (20) with acceptable accuracy $O(\varepsilon^4)$ for the stationary regime of modulation. The second and third relations here clearly show that the wave action flux of the side bands can grow up at the expense of the main carrier wave flux. The last relationship manifests the almost identical behavior of the main sidebands for the problem of their generation due to Benjamin-Feir instability.

Typical behavior of wave instability in the absence of current is presented in Fig. 1a for a Stokes wave having initial steepness $\varepsilon = 0.1$. Two initially negligible side bands (II) and (III) exponentially grow at the expense of the main Stokes wave (I), and after saturation, the wave system reverts to its initial state, which is the Fermi–Pasta–Ulam recurrence phenomenon. One can see here also the characteristic spatial scale for the developing of modulation instability $O(1/(k_c\varepsilon^2))$.

The development of modulation instability on negative variable current $U = U_0 Sech\left[\varepsilon^2(x-200)\right], U_0 = -0.1,$ is presented in Fig. 1(b). The modulation instability develops far more quickly on opposing current and reaches deeper stages of modulation. The energetic process is described as follows. The basic Stokes wave (I) absorbs energy from the counter current U and its steepness increases. This in turn accelerates the wave instability; there is a corresponding increase in energy flow to the most unstable sideband modes (II) and (III). The linear modulation model (Gargett & Hughes (1972), Lewis et al. (1974)) has much larger maximum amplitude of the carrier wave (IV).

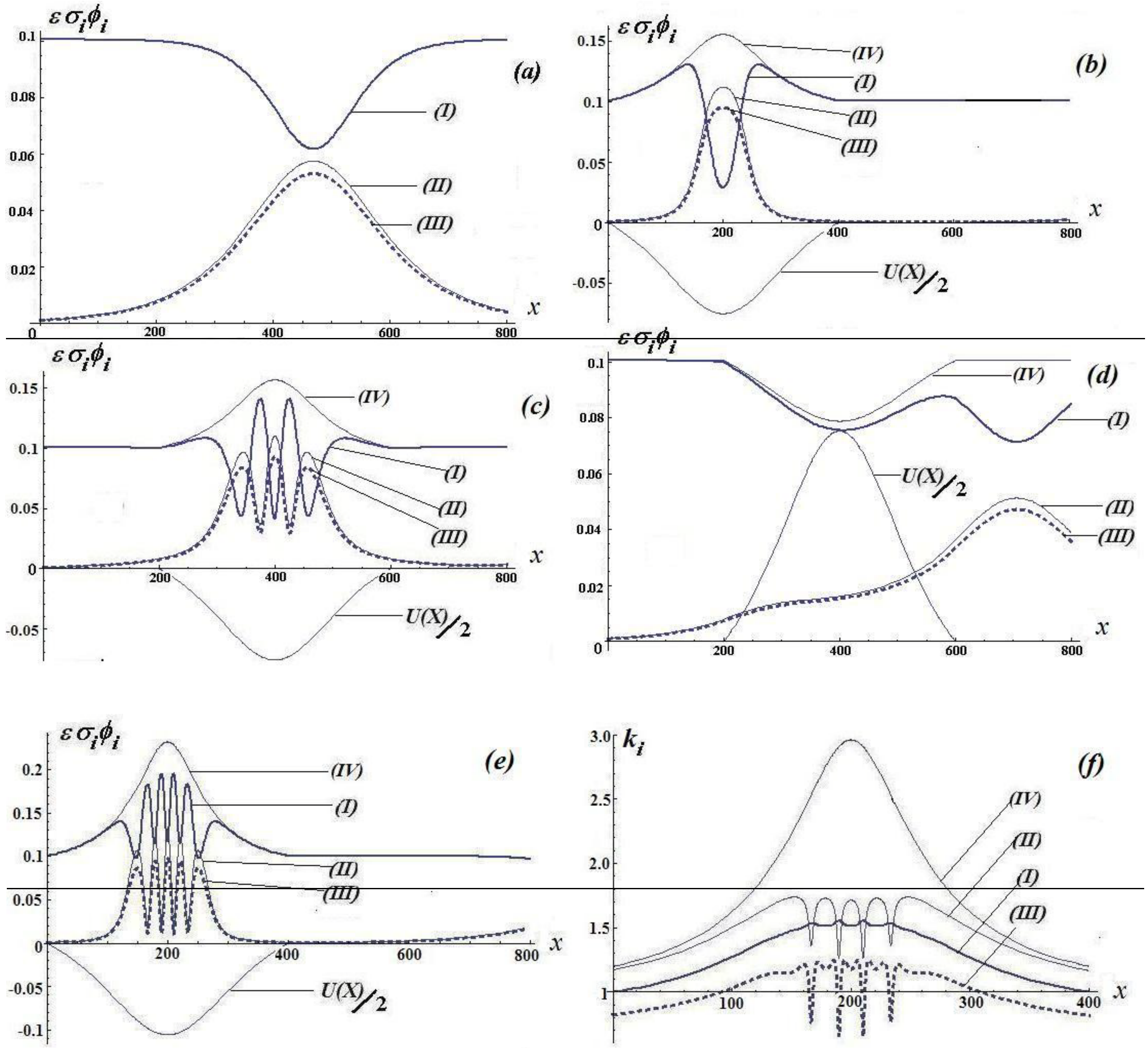

~~FIG. 1. (a) BF instability without current. (b), (c) Modulation of surface waves by adverse current $U = U_0 Sech\left[\varepsilon^2(x - x_0)\right]$, ($U_0 = -0.1$); (b) $x_0 = 200$, (c) $x_0 = 400$. (d) Modulation instability for following current ($U_0 = 0.1$, $x_0 = 400$). (e), (f) Functions of wave amplitude and wave number respectively for $U_0 = -0.2$. (I), (II), (III) Amplitude envelopes of the carrier, superharmonic and subharmonic waves, respectively. (IV) Linear solution for the carrier envelope. The initial steepness of the carrier wave is $\varepsilon = 0.1$.~~

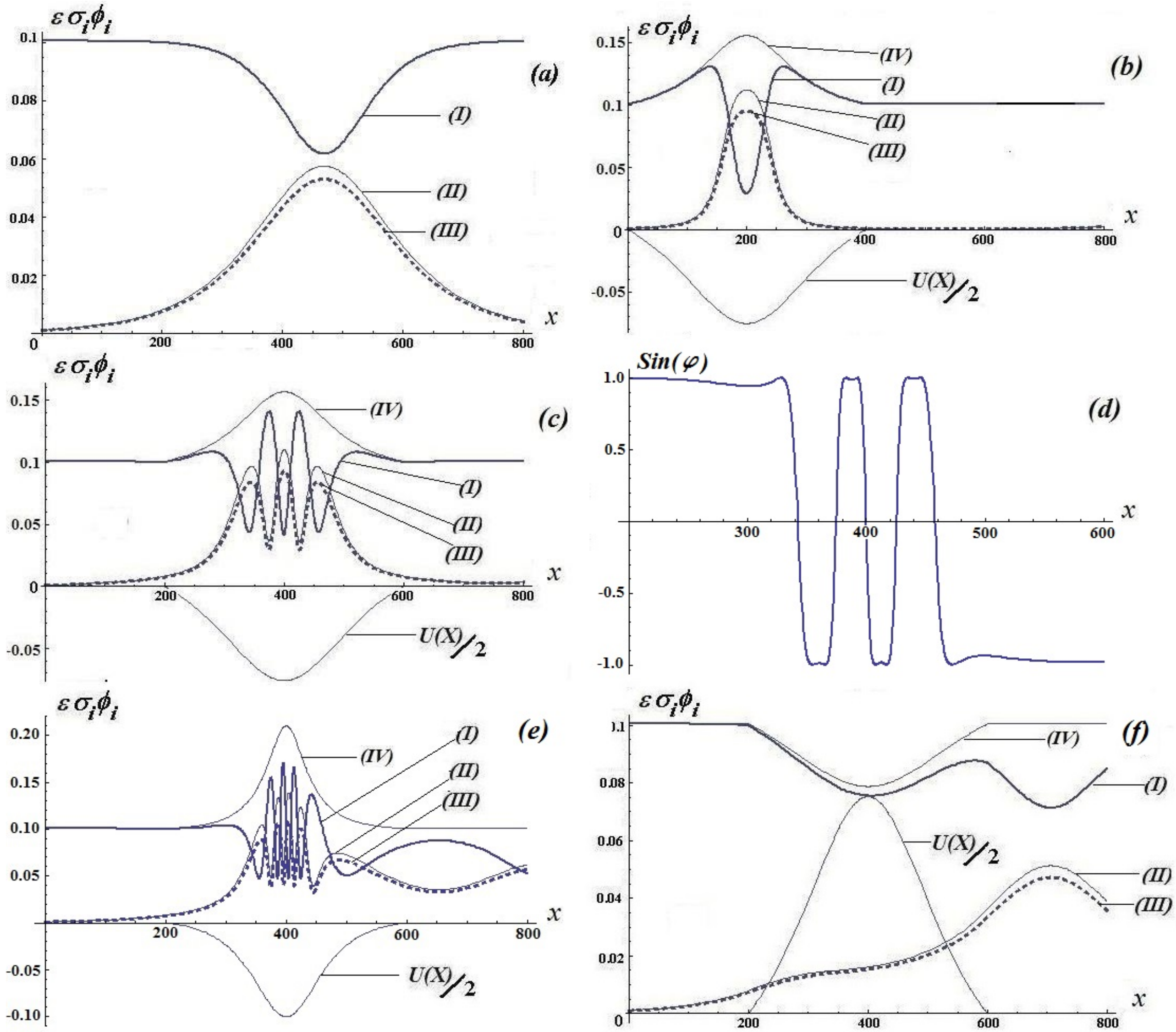
(a)
(b)
(c)
(d)
(e)
(f)
(I)
(II)
(III)
(IV)
U(X)/2
Sin(φ)
x

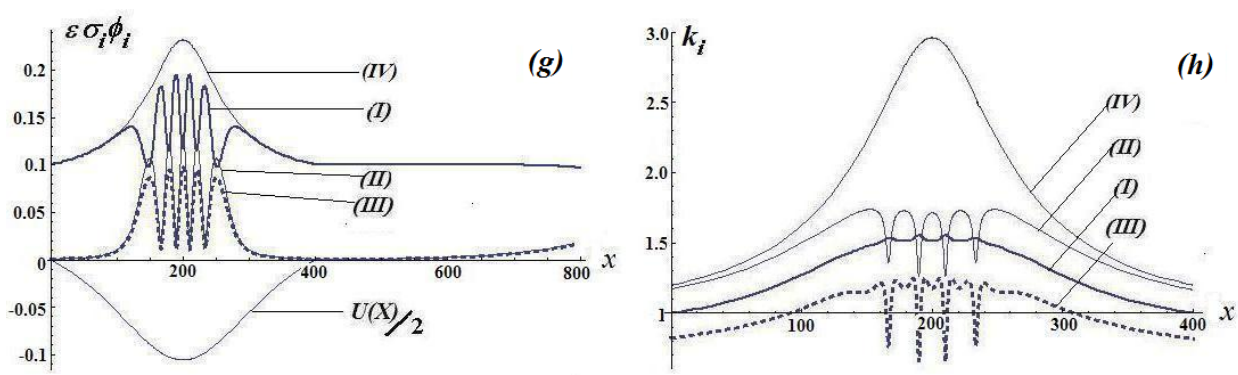
(g)
(h)
(I)
(II)
(III)
(IV)
U(X)/2
x

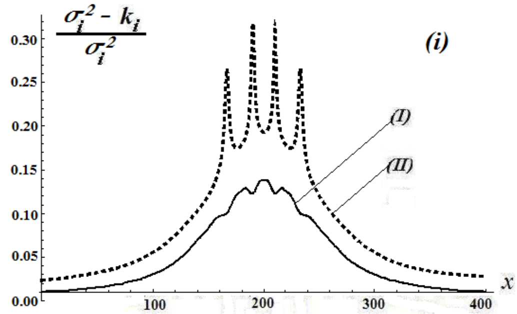

FIG. 1. (a) BF instability without current. (b), (c) Modulation of surface waves by adverse current $U = U_0 Sech\left[\varepsilon^2 (x - x_0)\right]$, ($U_0 = -0.15$); (b) $x_0 = 200$, (c) $x_0 = 400$. (d) phase difference function $\varphi[X] = 2\theta_1[X] - \theta_0[X] - \theta_2[X]$, $\theta_1[0] = 0; \theta_0[0] = \theta_2[0] = -\pi/4$, (e) Modulation of surface waves by adverse current $U = U_0 Sech\left[2\varepsilon^2 (x - x_0)\right]$, ($U_0 = -0.2$), (f) Modulation instability for following current ($U_0 = 0.16$, $x_0 = 400$). (g), (h) Functions of wave amplitude and wave number respectively for $U_0 = -0.2$. (I), (II), (III) Amplitude envelopes of the carrier, superharmonic and subharmonic waves, respectively. (IV) Linear solution for the carrier envelope. The initial steepness of the carrier wave is $\varepsilon = 0.1$, side band initial amplitudes are equal to 0.1ε . (i) Relative distortion of the linear dispersion relation for the case (g), (I) – carrier, (II) – higher side band.

The region of the most developed instability corresponds to the spatial location of the maximum of the negative current (Fig. 1c). ~~The counter energy flows from the current and the other resonant waves give rise to mutual oscillations for all wave amplitudes (I)–(III).~~ As one can see from Fig. 1b, 1c the initial stage of wave-current interaction is characterized by the dominant process - absorbing of energy by waves where all three waves grow simultaneously. Initial growth of side band modes (Fig.1c) leads to more deep modulated regime. Increasing of wave steepness in turn accelerates instability and finally these two dominate processes alternate. Correspondingly, the triggering of this complicate process essentially depends from the displacement of the current maximum.

Quasi-resonance interaction of waves in the presence of variable current causes some crucial questions about its detuning properties. Absolute frequencies for the stationary modulation satisfy to resonance conditions (7) for the entire region of interaction. But possibly it is not the case for the local wave numbers and intrinsic frequencies - they are substantially variable due to current effects and nonlinearity. May be due to interaction with current and nonlinearity effects the almost resonance conditions are totally destroyed due to large detuning? (Shrira and Slunyaev, 2014)

To clarify this property we present the Fig.1d describing the typical behavior of phase-shift difference function $\varphi[X] = 2\theta_1 - \theta_0 - \theta_2$ corresponding to wave modulation at Fig.1c. Intensity of nonlinear energy transfer is mostly defined by this function together with wave amplitudes. (see equations (17), (20)). Result looks rather surprising - several strong phases' jumps take a place with corresponding changing of the wave energy fluxes direction. But in any case we see an intensive quasi-resonant energy exchange in the entire interaction zone. Quasi-resonant conditions are satisfied locally in space with a relatively small detuning factor. Qualitatively similar behavior of phase-shift function we found also for other regimes of wave modulation.

The ~~opposite~~ typical scenario of wave interaction with copropagating current is presented in Fig. 1f. The modulation instability is depressed by the following current $U(X) > 0$ and the resonant sideband modes develop at a distance from the origin that is almost twice that in the case of no current.

Regimes of modulation presented at Fig. 1a-1c demonstrate the strictly symmetrical behavior with respect to the current peak and wave train returns to its initial structure after interaction with current. The modulation equations permit symmetrical solutions for the symmetrical current function, but, in general, outside of interaction zone the structure of nonlinear periodic waves are defined by the boundary conditions and constant Stokes wave is only one of such possibilities. The symmetrical behavior is typical for a sufficiently long scale current. We present Fig.1e with the asymmetrical modulation properties for the same wave initial characteristics as for Fig.1c and two time's shorter space scale of the current. After wave-current interaction zone we see three waves system with comparable amplitudes and periodic energy transfers.

The increasing strength of the opposing flow ($U_0 = -0.2$) results in deeper modulation of waves and more frequent mutual oscillations of the amplitudes (Fig. 1g). There are essential oscillations of wave-number functions of the sideband modes (II) and (III) (Fig. 1h) owing to the nonlinear dispersion properties of waves. We mention also that the wave number of the carrier wave in the linear model (IV) is much higher than that in the nonlinear model (I). The width of the wave-number spectrum of the wave train in the nonlinear model locally increases to almost twice the initial width. To give an idea about the strength of nonlinearity we present at Fig.1i the distortion of the linear dispersion relation for different modes. As one can see the effect of nonlinearity for the carrier (at maximum is about 10%) is much less compare to side bands (at peak is more than 30 %). The main impact of nonlinearity comes from amplitude Stokes dispersion.

To estimate the possibility of generating large transient waves, we employ the resonance model and calculate the maximum amplification of the amplitudes of surface waves ~~on linearly increasing opposing current~~ generated in a still water and then undergo a current quickly raised to a constant value

$-U$. The boundary conditions for the unperturbed waves were taken from experiments conducted by Toffoli et al. (2013) and Ma et al. (2013). Results of calculations are presented in Fig. 2(a) and 2(b).

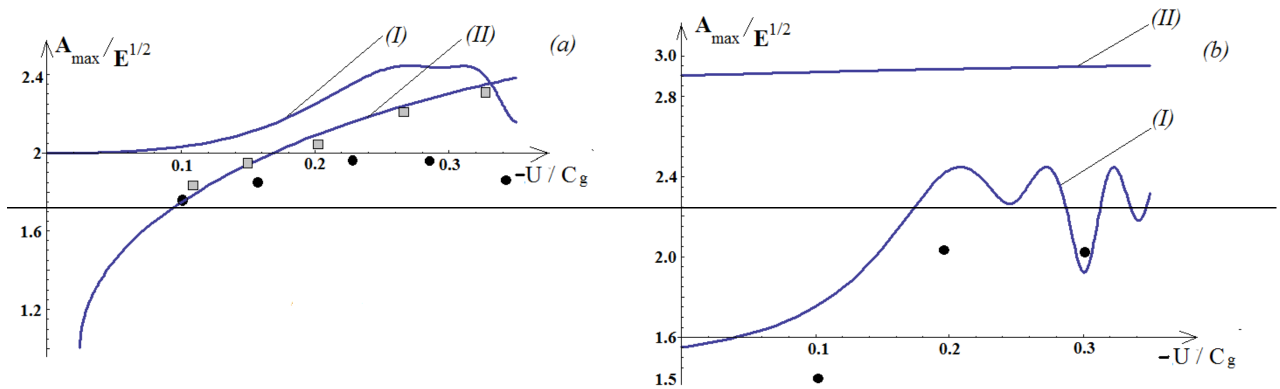

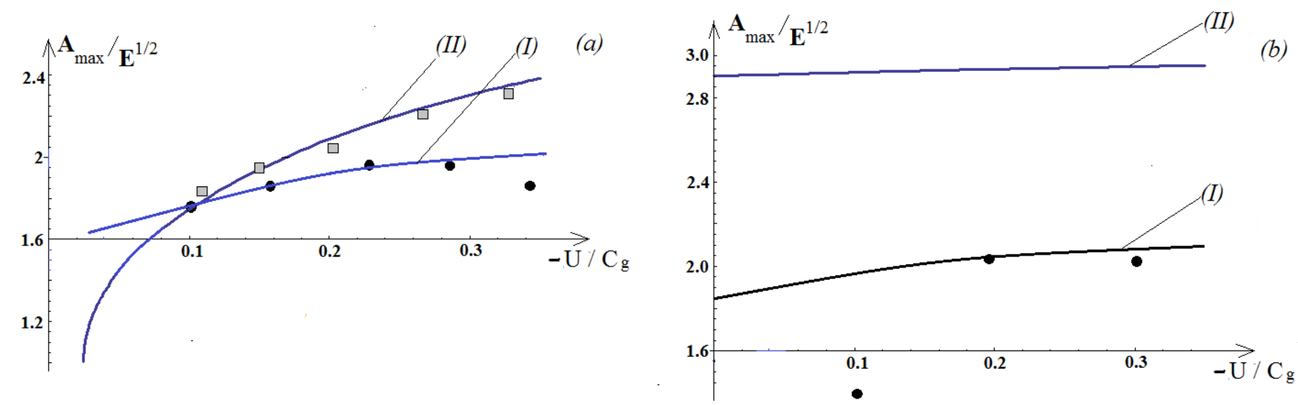

FIG. 2. Nondimensional maximum wave amplitude as a function of $-U/C_g$, where C_g is the group velocity of the carrier wave and $E^{1/2}$ is the local standard deviation of the wave envelope.

(a) Experiments conducted by Toffoli et al. (2013) for carrier wave of period $T = 0.8s$ (wavelength $\lambda \cong 1m$), initial steepness $k_1 a_1 = 0.063$, and frequency difference $\Delta\omega/\omega_1 = 1/11$, initial amplitudes of side bands equal to 0.25 times the amplitude of the carrier wave. Solid dots show measurements made using a flume at Tokyo University and squares show results obtained at Plymouth University. Line (I) shows the resonance model prediction while line (II) shows the prediction made using Eq. (2) (Toffoli et al., 2013).

(b) Case T11 in Ma et al. (2013) for carrier-wave frequency $\omega_1 = 1Hz$, initial steepness $k_1 a_1 = 0.115$, initial amplitudes of side bands equal to 0.05 times the amplitude of the carrier wave and frequency difference $\Delta\omega/\omega_1 = 0.44 a_1 k_1$. Solid dots show measurements. Line (I) shows the resonance model prediction, while line (II) shows the prediction made using Eq. (2) (Toffoli et al., 2013).

~~Qualitatively, the results of both tests conducted by Toffoli et al. (2013) (Fig. 2 (a)) are in good agreement with the theory presented by Onorato et al. (2011). The resonant model slightly overestimates the experimental values. However, observations made by Ma et al. (2014) (Fig. 2(b)) are notably overestimated by the theory of Onorato et al. (2011) and resonance-model simulations are in far greater agreement with the experimental values.~~

Our simulations confirm that initially stable waves in experiments of Toffoli et al. (2013) undergo a modulationally unstable process and wave amplification in the presence of adverse current. Maximum amplification reasonably corresponds to results of experiments in Tokyo University Tank for moderate strength of current. Maximum of nonlinear focusing in dependence on the value of current is weaker compare to the model of Toffoli et al.(2013).

Experiments of Ma et al. (2013) (Fig. 2b) show that the development of the modulational instability for a gentle waves and relatively weak adverse current ($U/C_g \sim -0.1$, see the first experimental point) is limited due to the presence of dissipation. Our resonance-model simulations are in a good agreement with the experimental values for the moderate values of adverse current $U/C_g \sim -0.2-0.4$. Results of Toffoli et al. (2013) notably overestimate the maximum of wave amplification.

4. Wave propagation under the blocking conditions of strong adverse current

Stokes waves with sufficiently high initial steepness ε under the impact of strong blocking adverse current ($U(X) < -C_g$) will inevitably reach the breaking threshold for the steepness of water waves. We include breaking dissipation effects in this case. We employ the adjusted dissipative model of Tulin (1996) and Huang et al. (2011) to describe the effect of breaking on the dynamics of the water wave. An analysis of fetch laws parameterized by Tulin reveals that the rate of energy loss due to breaking is of fourth order of the wave amplitude:

$$D_a / e = \omega D \eta^2 k^2 \,,$$

where e is the wave energy density and $D = O(10^{-1})$ is a small empirical constant.

The sinks of energy and momentum terms for each of the waves are calculated in accordance with the dissipative Schrodinger model for the complex amplitude $A \sim \sum \phi_t e^{i\theta_i}$ ::

$$A_T + C_g A_X + i\frac{C_g}{4k} A_{XX} + \frac{i}{2}\omega k^2 |A|^2 A = \left(-\frac{DA}{g|A|^2} - 4i\gamma A \int \frac{\omega^2 D dX}{g|A|^2} \right) H\left[\frac{|A_X|}{A_S} - 1 \right]$$

where $D \sim gD_b|A|^4$, $D_b = O(10^{-1}), \gamma = O(10^{-1})$ - constants of proportionality taken from the field observations, g – gravity acceleration, H is the Heaviside unit step function, and A_S is the threshold value of the characteristic steepness $A_X = \varepsilon \sum \sigma_i \phi_i k_i$. Right side part leads to additional terms in the governing modulation equations (16), (17), (20).

~~The sink of energy and momentum due to wave breaking leads to additional terms on the right sides of the wave energy equations (20) and dispersive equations (16) for each wave.~~ Tulin (1996) suggested using sink terms along the entire path of wave interaction with the wind. The wave dissipation function for the adjusted model (Huang et al., 2011) includes also the wave steepness threshold function

$$H\left[\frac{|A_X|}{A_S} - 1\right],$$

applied to calculate energy and momentum losses in a high steepness zones.

The dispersion relations (16) and wave energy laws (20) including break dissipation take the form

$$\begin{cases}
\sigma_0{}^2 = k_0 + \varepsilon^2\sigma_0{}^3(\phi_0^2\sigma_0{}^5 + \phi_1^2\sigma_1{}^3(2\ \sigma_1{}^2 - \sigma_0\sigma_1 + \sigma_0{}^2) + \phi_2^2\sigma_2{}^3(2\sigma_2{}^2 - \sigma_0\sigma_2 + \sigma_0{}^2)) + \\
\dfrac{\varepsilon^2\phi_1^2\phi_2\sigma_1{}^3\sigma_2{}^2}{\phi_0}(2\sigma_1{}^3 - 2\sigma_1{}^2\sigma_2 + 2\ \sigma_1\sigma_2{}^2 - \sigma_2{}^3)\cos[\varphi] + \varepsilon^2 \mathrm{H}[\chi]\begin{Bmatrix} DSin[\varphi]\phi_1^2\phi_2/\phi_0 \mathrm{k}_0^4 + 8\gamma D\varepsilon^2 \mathrm{X}(\phi_0{}^2 + \phi_1{}^2 + \phi_2{}^2) - \\ 4\gamma \mathrm{D}\phi_1{}^2\phi_2/\phi_0 \sin[\varphi]\varepsilon/(\mathrm{k}_2 - \mathrm{k}_1) \end{Bmatrix}; \\
\\
\sigma_2{}^2 = k_2 + \varepsilon^2\sigma_2{}^3(\phi_2^2\sigma_2{}^5 + \phi_0^2\sigma_0{}^3(2\sigma_0{}^2 - \sigma_0\sigma_2 + \sigma_2{}^2) + \ \phi_1^2\sigma_1{}^3(2\sigma_1{}^2 - \sigma_1\sigma_2 + \sigma_2{}^2)) + \\
\dfrac{\varepsilon^2\phi_1^2\phi_0\sigma_1{}^3\sigma_0{}^2}{\phi_2}(2\sigma_1{}^3 - 2\ \sigma_0\sigma_1{}^2 + 2\sigma_0{}^2\sigma_1 - \sigma_0{}^3)\cos[\varphi] + \varepsilon^2 \mathrm{H}[\chi]\begin{Bmatrix} DSin[\varphi]\phi_1^2\phi_0/\phi_2 \mathrm{k}_2^4 + 8\gamma D\varepsilon^2 \mathrm{X}(\phi_0{}^2 + \phi_1{}^2 + \phi_2{}^2) + \\ 4\gamma \mathrm{D}\phi_1{}^2\phi_0/\phi_2 \sin[\varphi]\varepsilon/(\mathrm{k}_1 - \mathrm{k}_0) \end{Bmatrix}; \\
\\
\sigma_1{}^2 = k_1 + \varepsilon^2\sigma_1{}^3(\phi_1^2\sigma_1{}^5 + \phi_0^2\sigma_0{}^3(2\ \sigma_0{}^2 - \sigma_0\sigma_1 + \sigma_1{}^2) + \phi_2^2\sigma_2{}^3(\sigma_1{}^2 - \sigma_1\sigma_2 + 2\sigma_2{}^2)) + \\
\varepsilon^2\phi_0\ \ \phi_2\sigma_0\sigma_1{}^2\sigma_2(\sigma_0{}^4 - \sigma_0{}^3\sigma_1 - \sigma_0\sigma_1(\sigma_1 - \sigma_2)^2 + \ \sigma_0{}^2(\sigma_1{}^2 - \sigma_1\sigma_2 + 2\sigma_2{}^2) + \\
\sigma_2(-\sigma_1{}^3 + \sigma_1{}^2\sigma_2 - \sigma_1\sigma_2{}^2 + \sigma_2{}^3))\cos[\varphi] + \varepsilon^2 \mathrm{H}[\chi]\begin{Bmatrix} -2D\sin[\varphi]\phi_2\phi_0 \mathrm{k}_1^4 + 8\gamma D\varepsilon^2 \mathrm{X}(\phi_0{}^2 + \phi_1{}^2 + \phi_2{}^2) + \\ 4\gamma \mathrm{D}\phi_2\phi_0 \sin[\varphi]\dfrac{(\mathrm{k}_2 - 2\mathrm{k}_1 + \mathrm{k}_0)2\varepsilon}{(\mathrm{k}_1 - k_0)(\mathrm{k}_2 - k_1)} \end{Bmatrix};
\end{cases} \quad (21)$$

where $\chi = |A_X|/A_S - 1$, and

$$
\begin{cases}
[(U(X)+\frac{1}{2\sigma_0})\phi_0^2\sigma_0^2]_X = \varepsilon\phi_1^2\phi_2\phi_0\sigma_1{}^3\sigma_2{}^2(2\sigma_1{}^3\text{-}2\sigma_1{}^2\sigma_2\text{+}2\ \sigma_1\sigma_2{}^2\text{-}\sigma_2{}^3)\sin[\varphi]\text{-}\phi_0^2\sigma_0 U'(X)/2\text{+}\varepsilon \mathrm{H}[\chi]\begin{Bmatrix} \text{-}\mathrm{k}_0^4\phi_1^2\phi_2\phi_0 D\cos[\varphi]-\mathrm{k}_0^4\phi_0{}^2(\phi_0{}^2+2\phi_1{}^2+2\phi_2{}^2)+ \\ 4\gamma D\phi_0{}^2 k_0^4(\phi_1{}^2\varepsilon/(k_1-k_0)+\phi_2{}^2 2\varepsilon/(k_2-k_0)+ \\ \phi_1{}^2\phi_2/\phi_0\cos[\varphi]\varepsilon/(k_2-k_1)) \end{Bmatrix}; \\
[(U(X)+\frac{1}{2\sigma_2})\phi_2^2\sigma_2^2]_X = \varepsilon\phi_1^2\phi_2\phi_0\sigma_1{}^3\sigma_0{}^2(2\sigma_1{}^3\text{-}2\sigma_0\sigma_1{}^2\text{+}2\sigma_0{}^2\sigma_1\text{-}\sigma_0{}^3)\sin[\varphi]\text{-}\phi_2^2\sigma_2 U'(X)/2\text{+}\varepsilon \mathrm{H}[\chi]\begin{Bmatrix} \text{-}\mathrm{k}_2^4\phi_1^2\phi_2\phi_0 D\cos[\varphi]-\mathrm{k}_2^4\phi_2{}^2(\phi_2{}^2+2\phi_0{}^2+2\phi_1{}^2)+ \\ 4\gamma D\phi_2{}^2 k_2^4(\phi_1{}^2\varepsilon/(k_2-k_1)+\phi_0{}^2 2\varepsilon/(k_2-k_0)+ \\ \phi_1{}^2\phi_0/\phi_2\cos[\varphi]\varepsilon/(k_1-k_0)) \end{Bmatrix}; \\
[(U(X)+\frac{1}{2\sigma_1})\phi_1^2\sigma_1^2]_X = -\varepsilon\phi_1^2\phi_2\phi_0\sigma_0\sigma_1{}^2\sigma_2(\sigma_0{}^4-\sigma_0{}^3\sigma_1-\sigma_0\sigma_1(\sigma_1\text{-}\sigma_2)^2+\sigma_0{}^2(\sigma_1{}^2\text{-}\sigma_1\sigma_2\text{+}2\sigma_2{}^2)\text{-}\sigma_2(\sigma_1{}^3\text{-}\sigma_1{}^2\sigma_2\text{+}\sigma_1\sigma_2{}^2\text{-}\sigma_2{}^3))\sin[\varphi] \\
\text{-}\phi_1^2\sigma_1 U'(X)/2\text{+}\varepsilon \mathrm{H}[\chi]\begin{Bmatrix} \text{-}2\mathrm{k}_1^4\phi_1^2\phi_2\phi_0 D\cos[\varphi]-\mathrm{k}_1^4\phi_1{}^2(\phi_1{}^2+2\phi_0{}^2+2\phi_2{}^2)+ \\ 4\gamma D\phi_1{}^2 k_1^4((\phi_2{}^2-\phi_0{}^2)\varepsilon/(k_1-k_0)+ \\ \phi_2\phi_0\cos[\varphi](k_2+k_0-2k_1)/(k_2-k_1)\varepsilon/(k_2-k_1)) \end{Bmatrix};
\end{cases}
\tag{22}
$$

where empirical constant $\gamma = O(10^{-1})$.

The terms $\varepsilon/(k_i-k_j)$ appear in the right side of equations due to integration procedure and have an order of unit. The singularity was not detected in numerical simulations.

Wave breaking leads to permanent (not temporal) frequency downshifting at a rate controlled by breaking process. A crucial aspect here is the cooperation of dissipation and near-neighbor energy transfer in the discretized spectrum acting together.

The numerical simulations for initially high steepness waves ($\varepsilon = 0.25$) propagation with wave breaking dissipation is presented in Fig. 3a-3c. We calculate the amplitudes of surface waves on linearly increasing opposing current $U(x) = -U_0 x$ with different strength U_0. Most unstable regime was tested for frequency space $\Delta\omega_{\pm}/\omega_1 \sim \varepsilon$, initial side bands amplitudes equal to 0.05 times the amplitude of the carrier wave and most effective initial phases $\theta_1(0)=0, \theta_0(0)=\theta_2(0)=-\pi/4$

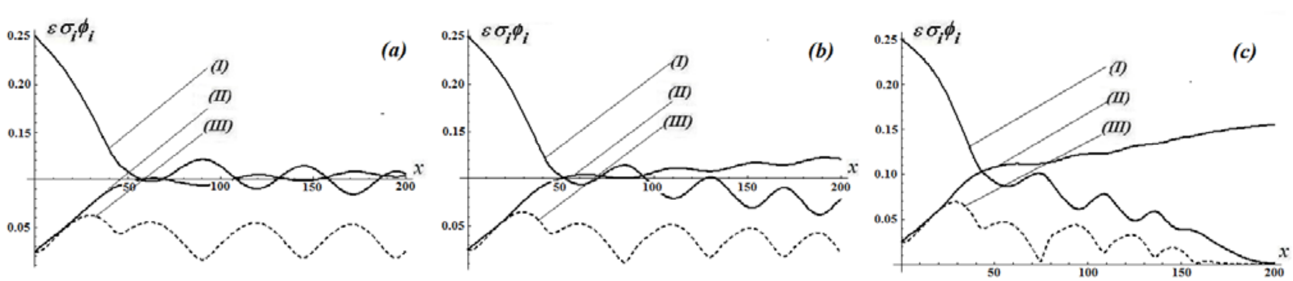

FIG. 3. Modulation of surface waves by the adverse current $U = U_0 x$. (a) $U_0 = -2.5\ 10^{-4}$; (b) $U_0 = -5\ 10^{-4}$, (c) $U_0 = -10^{-3}$. (I), (II), (III) - amplitude envelopes of the carrier, subharmonic and superharmonic waves, respectively. Initial wave steepness $\varepsilon = 0.25$, side bands amplitudes equal to 0.05 times the amplitude of the carrier, dissipation parameters $D_b = 0.1, \gamma = 0.5$

A very weak opposite current $U_0 = 2.5\ 10^{-4}$ (Fig.3a) has a pure impact on wave behavior: it is finally results in almost bichromatic wave train with two dominant waves: carrier and lower side band.

Frequency downshift here is not clearly seen. Two times stronger current case with $U_0 = 5\ 10^{-4}$ is presented in Fig. 3b. We note some tendency to final energy downshift to the lower side band. Really strong permanent downshift with total domination of the lower side band is seen for two times more strong current $U_0 = 10^{-3}$ (Fig.3c).

We also performed numerical simulations ~~using the model~~ for the boundary conditions and the form of the variable current obtained in two series of experiments conducted by Chavla and Kirby (2002) and Ma et al. (2010).

Data for the wave blocking regime in experiments conducted by Chavla and Kirby (2002) are taken from their Test 6 (Figure 11). The experimental results of Test 6 and our numerical simulation results are compared in Fig. 4. A surface wave with initially high steepness ($A_1 k_1 = 0.296$) and period T = 1.2 s meets adverse current with increasing amplitude.

The wave modeling has distinctive features that agree reasonably well with the results of experiments:

- initial symmetrical growth of the main sidebands with frequencies $f_0 = 0.688 Hz, f_2 = 0.978 Hz$ at distances up to $k_1 x < -2$;

- asymmetrical growth of sidebands beginning at $(k_1 x \approx -2)$ and downshifting of energy to the lower sideband;

- energy transfer at very short spatial distances and several increases in the lower sideband amplitude just on a half meter length $k_1 x \in (-2, 0)$.

- a depressed higher frequency band and primary wave;

- an almost permanent increase in the lowest subharmonic along the tank;

- sharp accumulation of energy by the lowest subharmonic wave during interaction with increasing opposing current; and

- final permanent downshifting of the wave energy.

The presented third-order wave amplitude model agrees reasonable well with experimental results.

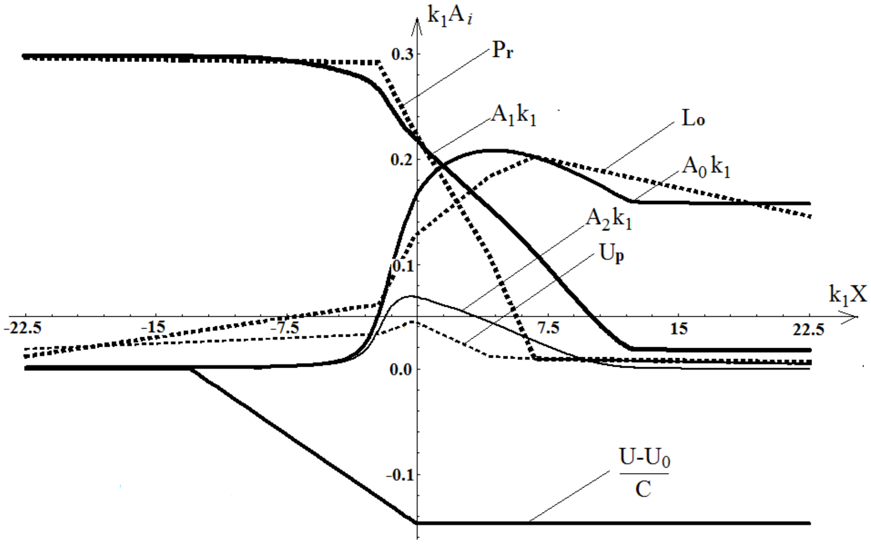

FIG. 4. Dashed curves show the zero-dimensional amplitudes of the resonance waves for primary (Pr), lower (Lo) and upper (Up) sidebands obtained experimentally by Chavla and Kirby (2002). The solid lines (A_1, A_0, A_2 respectively) are wave amplitudes calculated in modeling. $(U-U_0)/C$ is the zero-dimensional variable current, where C is the initial phase speed of the carrier wave, $U_0 = -0.32 m/s; k_1 = 4.7\ 1/m, C = 1.44 m/s, T = 1.2 s$.

Modulation evolution of breaking waves in experiments of Ma et al. (2010) for the most intriguing case 3 are presented in Fig.5 together with the results of our numerical computations. A primary wave with period $T = 1s$ and steepness $A_1 k_1 = 0.18$ meets linearly increasing opposing current that finally exceeds the threshold to be a linear blocking barrier for the primary wave $U(x) < -1/4C$. In experiments, sideband frequencies arose ubiquitously from the background noise of the flume. In numerical simulations, the sidebands were slightly seeded at frequencies corresponding to the most unstable modes. The wave-breaking region in this experimental case ranged from $k_1 x = 52$ to $k_1 x = 72$. The lower sideband amplitude grew with increasing distance at the expense of the primary wave, while there was little change in the higher sideband energy. There was an effective frequency downshift following initial breaking ($k_1 x = 56$). The modeling results agree reasonably well with the experimental data.

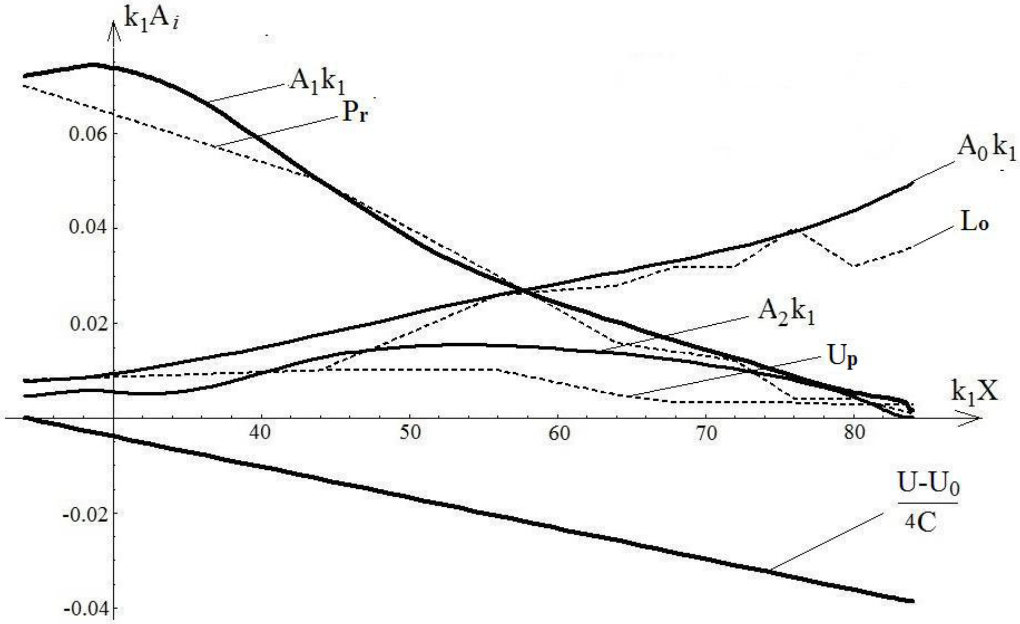

FIG. 5. Dashed curves show zero-dimensional amplitudes of the resonance waves for primary (Pr), lower (Lo) and upper (Up) sidebands obtained from experiments conducted by Ma et al. (2010). The solid lines (A_1, A_0, A_2 respectively) are wave amplitudes calculated in modeling. $(U-U_0)/(4C)$ shows the zero-dimensional variable current, where C is the initial phase speed of the primary wave, $U_0 = -0.25m/\mathrm{s}; k_1 = 4.\ 1/m, C = 1.56m/\mathrm{s}, T = 1\mathrm{s}$.

5. Conclusions

A resonance system comprising three waves in nonuniform media gives rise to modulation instability with special properties. Interaction with countercurrent accelerates the growth of sideband modes on much shorter spatial scales. In contrast, wave instability on following current is sharply depressed. Amplitudes and wave numbers of all quasi-resonant waves vary enormously in the presence of strong adverse current. The steepness of a nonlinear wave on adverse current is much less than that of a linear refraction model.

Large transient or freak waves with amplitude and steepness several times larger than those of normal waves may form during temporal nonlinear focusing of the quasi-resonant waves accompanied by energy income from sufficiently strong opposing current. The amplitude of a rough wave strongly depends on the ratio of the current velocity to group velocity.

Interaction of initially steep waves with the strong blocking adverse current results in intensive energy exchange between quasi-resonance components and energy downshifting to the lower sideband mode accompanied by active breaking. A more stable long wave with lower frequency can overpass the blocking barrier and accumulate almost all the wave energy of the packet. The frequency downshift of the energy peak is permanent and the system does not revert to its initial state.

A third-order dissipative wave resonant model satisfactorily agrees with available experimental data on the explosive instability of waves on blocking adverse current and the generation of rough waves.

Acknowledgements

The authors would like to thank the Ministry of Science and Technology of Taiwan (NSC 103-2911-I-006 -302 and to National Cheng-Kung University) and the Ministry of Education, Taiwan, R.O.C. The Aim for the Top University Project to the National Cheng Kung for financial support.

References

Benjamin, T. B. and Feir, J. E., “Instability of periodic wavetrains in nonlinear dispersive systems,” J. Fluid Mech.Vol. 27**,** 417-430, 1967.

Bridges, T., and Dias, F., “Enhancement of the Benjamin-Feir instability with dissipation,” Phys. Fluids, Vol. 19**,** 104104, 2007.

Chavla, A. and Kirby, J., “Experimental study of breaking waves on a blocking current,” Proc. 26th International Conference on Coastal Engineering, Copenhagen, June 22-26, 759-772, 1998.

Chavla, A. and Kirby, J. “Monochromatic and random wave breaking at block points,” Journal of Geophysical Res., Vol. 107, C7, 4.1-4.19, 2002.

Chabchoub, A., Akhmediev, N. and Hoffmann, N., **“**Experimental study of spatiotemporally localized surface gravity water waves,” Physical Review E. Vol. 86, 016311, 2012.

Chiang, W. and Hwung, H., “Large transient waves generated through modulational instability in deep water,”J. Hydrodynamics, 22(5), 114-119, 2010.

Dias, F., Kharif, C., “Nonlinear gravity and capillary-gravity waves,” Annu. Rev. Fluid Mech. Vol. 31, 301-346, 1999.

Donato, A. N., Peregrine, D. H. & Stocker, J. R. “The focusing of surface. waves by internal Waves,” J. Fluid Mech. Vol. 384, 27–58, 1999.

Duin, C., “The effect of non-uniformity of modulated wavepackets on the mechanism of Benjamin–Feir instability,” J. Fluid Mech., Vol. 399, 237–249, 1999.

Dysthe, K. B., “Note on a modification to the nonlinear Schrodinger equation for application to deep water waves,” Proc. R. Soc. A, Vol. 369, 105-114, 1979.

Gargett, A. E. and Hughes, B. A., “On the interaction of surface and internal waves,” J. Fluid Mech. Vol. 52, 179-191, 1972.

Gerber, M., “The Benjamin–Feir instability of a deep water Stokes wavepacket in the presence of a non-uniform medium,” J. Fluid Mech.Vol. 176, 311–332, 1987.

Hara, T. and Mei, C., ” Frequency downshift in narrowbanded surface waves under the influence of wind,” J. Fluid Mech., Vol. 176, 311–332, 1987.

Hjelmervik, K.B. and Trulsen, K., “Freak wave statistics on collinear currents,” J. Fluid Mech. Vol. 637, 267-284, 2009.

Hwung, H., Chiang W. and Hsiao S., “Observations on the evolution of wave modulation,” Proc. R. Soc. London, Ser. A, Vol. 463**,** 85-112, 2007.

Hwung, H., Yang, R. and Shugan, I., “Exposure of internal waves on the sea surface,” J. Fluid Mech. Vol. 626, 1-20, 2009.

Hwung, H., Chiang W., Yang, R. and Shugan, I., “Threshold Model on the Evolution of Stokes Wave Side-Band Instability,” Eur. J. Mech. B/Fluids, Vol. 30, 147-155, 2011.

Janssen, P. “Nonlinear four-wave interactions and freak waves,” J. Phys. Oceanogr., Vol. 33, 863–884, 2003.

Janssen, T. and Herbers, T., “Nonlinear Wave Statistics in a Focal Zone,” J. Phys. Oceanogr., Vol. 39, 1948–1964, 2009.

Kharif, C. and Pelinovsky, E., “Freak waves phenomenon: physical mechanisms and modelling.” In: Waves in Geophysical Fluids: CISM Courses and Lectures 489 (ed. J. Grue & K. Trulsen), pp. 107–172. Springer, 2006.

Lake, B. M. and Yuen, H. C., “A new model for nonlinear wind waves. Part 1. Physical model and experimental evidence,” J. Fluid Mech. Vol. 88, 33-62, 1978.

Landrini, M., Oshri, O., Waseda, T. and Tulin, M. P. “Long time evolution of gravity wave systems,” In Proc. 13th Intl Workshop on Water Waves and Floating Bodies (ed. A. J. Hermans), Alphen aan den Rijn, pp. 75-78, 1998.

Lavrenov, I. V., “The wave energy concentration at the Agulhas current off South Africa,” Nat. Hazards, Vol. 17, 117-127, 1998.

Lewis, J. E., Lake, B. M., and Ko, D. R., "On the interaction of internal waves and surface gravity waves," J. Fluid Mech. Vol. 63, 773-800, 1974.

Lo, E. and Mei, C. C., "A numerical study of water-wave modulation base on a higher-order nonlinear Schrodinger equation," J. Fluid Mech., Vol. 150, 395-416, 1985.

Longuet-Higgins, M. and Stewart, R., "Radiation stresses in water waves: a physical discussion, with applications," Deep-sea Res. Vol.11, 529-562, 1964.

Ma, Y, Dong, G, Perlin, M., Ma, X., Wang, G. and Xu, J. "Laboratory observations of wave evolution, modulation and blocking due to spatially varying opposing currents," J. Fluid Mech., Vol. 661, 108-129, 2010.

Ma, Y, Ma, X., Perlin, M. and Dong, G., "Extreme waves generated by modulational instability on adverse currents," Physics of Fluids,Vol. 25, 114109, 2013.

Mei, C., You, D. and Stiassnie, M., "Theory and Applications of Ocean Surface Waves,". World Scientific, Hackensack (N.J.) , 2009.

Melville, W., "Wave modulation and breakdown," J. Fluid Mech. Vol. 128, 489-506, 1983.

Moreira, R. and Peregrine. D., "Nonlinear interactions between deep-water waves and currents," J. of Fluid Mech., Vol. 691, 1- 25, 2012.

Onorato M., Proment D. and Toffoli A., "Triggering rogue waves in opposing currents," Physical Review Letters, Vol. 107, 184502, 2011.

Osborne A., "The random and deterministic dynamics of 'rogue waves' in unidirectional, deep-water wave trains," Marine Structures. Vol. 14, 275-293, 2001.

Osborne A., "Nonlinear Ocean Waves and the Inverse Scattering Transform," Elsevier, New York (2010).

Osborne, A. R., Onorato M, and Serio M., "The nonlinear dynamics of rogue waves and holes in deep-water gravity wave trains," Phys. Lett. A, Vol. 275, 386–393, 2000.

Peregrine D.H., "Interaction of water waves and currents," Adv. Appl. Mech., Vol. 16, 9-117, 1976.

Phillips, O.M., "Theoretical and Experimental Studies of Gravity wave interactions," Proc. R. Soc. Lond. A, Vol. 299, 104-119, 1967.

Phillips, O.M., "The Dynamics of the Upper Ocean," Cambridge University Press (1977).

Ruban, V., "On the Nonlinear Schrödinger Equation for Waves on a Nonuniform Current," JETP Letters, Vol. 95, No. 9, 486–491, 2012

Segur, H., Henderson, D., Hammack, J., Li, C.-M., Phei, D. and Socha, K. "Stabilizing the Benjamin–Feir instability," J. Fluid Mech., Vol. 539, 229-271, 2005.

Shemer, L., Kit, E. and Jiao, H., "An experimental and numerical study of the spatial evolution of unidirectional nonlinear water-wave groups," Physics of fluids, Vol. 14, N10, 3380-3390, 2002.

Shemer L. "On Benjamin-Feir instability and evolution of a nonlinear wave with finite-amplitude sidebands," Nat. Hazards Earth Syst. Sci., Vol. 10, 1-7, 2010.

Shrira, V. and Slunyaev,A.," Trapped waves on jet currents: asymptotic modal approach,"J. Fluid Mech., Vol. 738, 65-104, 2014.

Shugan, I. and Voliak, K., "On phase kinks, negative frequencies and other third order peculiarities of modulated surface waves," J. Fluid Mech. Vol. 368, 321-338, 1998.

Slunyaev,A. and Shrira, V.,"On the highest non-breaking wave in a group: fully nonlinear water wave breathers versus weakly nonlinear theory,"J. Fluid Mech., Vol. 735, 203-248, 2013.

Smith, R., "Reflection of short gravity waves on a non-uniform current," Math. Proc. Cambridge Philos. Soc., Vol. 78, 517-525, 1975.

Stiassnie, M. and Shemer, L., "On the interaction of four water-waves," Wave Motion, Vol. 41, 307-328, 2005.

Stocker, J. R. and Peregrine, D. H., "Three-dimensional surface. waves propagating over long internal waves," European J. Mech. B/Fluids, Vol. 18, 545-559, 1999.

Tanaka, M., "Maximum amplitude of modulated wavetrain," Wave Motion, Vol. 12, 559-568, 1990.

Toffoli, A., Waseda, T. Houtani, H., Kinoshita T., Collins K., Proment D. and Onorato M., "Excitation of rogue waves in a variable medium: An experimental study on the interaction of water waves and currents," Physical Review E, Vol. 87, 051201, 2013.

Trulsen,K., and Dysthe, K. "Frequency down-shift through self modulation and breaking", In Water Wave Kinematics (ed. A. Torum & T. Gudmestad), 561-572, Kluwer (1990).

Trulsen,K., Kliakhandler, I., Dysthe, K. and Velarde M., "On weakly nonlinear modulation of waves on deep water," Physics of Fluids, Vol. 12**,** 2432–2437, 2000.

Tulin, M. P., "Breaking of ocean waves and downshifting," In Waves and Nonlinear Processes in Hydrodynamics (ed. J. Grue, B. Gjevik & J. E. Weber), 177-190. Kluwer, 1996.

Tulin, M. P. and Waseda, T., "Laboratory observations of wave group evolution, including breaking effects," J. Fluid Mech., Vol. 378,197-232, 1999.

White, B. & Fornberg,B., "On the chance of freak waves at sea," J. Fluid Mech., Vol. 355,113-138, 1998.

Whitham, G. B., "Linear and Nonlinear Waves," John Wiley & Sons, 1974.

Yuen, H. C. and Lake, B. M., "Nonlinear dynamics of deep-water gravity waves," In Advances in Applied Mechanics, Vol. 22, pp. 67–229. Academic Press, 1982.

Ying,L., Zhuang, Z., Heller E. and Kaplan, L., “Linear and nonlinear rogue wave statistics in the presence of random currents,”Nonlinearity, Vol. 24, R67-R87, 2011.

Zakharov, V., Dyachenko, A.and Prokofiev, A., “Freak waves as nonlinear stage of Stokes wave modulation instability,” European J. Mech. B/Fluids, Vol. 25, 677-692, 2006.